



Slab segmentation, anomalous arc volcanism, and giant porphyry copper deposits in Indonesia

Jack F. Ward^{a,*}, Gideon Rosenbaum^a, Teresa Ubide^a, Mike Sandiford^b

^a School of the Environment, The University of Queensland, Brisbane, QLD 4072, Australia

^b School of Geography, Earth and Atmospheric Sciences, The University of Melbourne, Carlton, Victoria 3053, Australia



ARTICLE INFO

Editor: Dr R. Hickey-Vargas

Keywords:

Subduction zone geodynamics
Arc volcanism
Ocean island basalt
Slab tear
Porphyry ore deposit
Critical minerals

ABSTRACT

Most Holocene volcanoes in Indonesia display geochemical and geophysical properties characteristic of formation via mantle wedge metasomatism. However, some volcanoes (Toba, Ungaran, Muriah, Rinjani, Tambora, Sangeang Api, and Batu Tara) are anomalous, showing alkaline geochemical affinities, anomalously violent recent eruptions, and/or positioning above sections of slab generally considered too deep to induce mantle melting via slab dehydration. These anomalous volcanoes are spatially and temporally associated with giant Pliocene–recent porphyry Cu deposits (in thin continental or oceanic crust), contrary to global occurrences of porphyry Cu deposits that are typically restricted to thick (>45 km crustal thickness) continental arcs. Using geophysical data to model slab geometry and geochemical data to evaluate source compositions and melting mechanisms, we demonstrate that anomalous Indonesian volcanoes and giant porphyry Cu deposits are linked to slab segmentation due to slab tearing. In the slab beneath Toba, the mechanically weak Investigator Fracture Zone, which separates a more buoyant Cenozoic segment of the Indo-Australian plate from older, denser, and more steeply dipping Jurassic–Cretaceous lithosphere to the east, likely created a sub-vertical slab tear feeding volcanism via poloidal mantle flow. The alkaline volcanoes Muriah, Ungaran, Tambora, and Sangeang Api (as well as the sub-alkaline volcano Rinjani) are positioned along edges of slab segments defined by negative seismic velocity anomalies at depths of ~185–400 km, which we interpret as elongate slab windows formed during localised choking of subduction by anomalously buoyant oceanic lithosphere. Although no negative velocity anomalies are associated with Batu Tara, we speculate that this alkaline volcano is located above a small-scale slab tear, potentially associated with the subducted Scott Plateau. We propose that poloidal asthenospheric flow along slab segment boundaries has triggered deep, low-degree partial melting with varying contributions of slab melt, sediment, and fluid. Products of this melting regime are sub-alkaline and alkaline lavas with trace element patterns enriched in incompatible elements relative to the main arc volcanoes. Based on spatial, temporal, and geochemical associations of giant Pliocene–recent porphyry Cu deposits with proposed slab tears (and an absence of evidence for slab melting in the formation of these deposits), we suggest that slab tears may have generated oxidised magmas by facilitating melting in the garnet stability field, emulating the petrogenetic effects of thick continental crust and slab melting. We further hypothesise that slab tearing locally enhanced magma flux, leading to extremely violent Quaternary eruptions at Toba, Rinjani, and Tambora.

1. Introduction

The generation of arc magma is typically ascribed to mantle wedge metasomatism, which occurs when subducted slabs dehydrate at depths of 90–150 km (Schmidt and Poli, 1998). Mantle wedge metasomatism produces sub-alkaline volcanic rocks that, when normalised to primitive mantle and mid-ocean ridge basalt (MORB) compositions, display enrichments of fluid-mobile large ion lithophile elements (LILEs; e.g., Ba,

Rb, Sr, and Pb) and depletions of fluid-immobile high field strength elements (HFSEs; e.g., Nb, Ta, Zr, and Hf; McCulloch and Gamble, 1991). In the Sunda and Banda arcs of Indonesia, most Holocene volcanoes exhibit typical arc signatures and are located in areas where the depth of the Indo-Australian slab is between 90 and 150 km (Figs. 1,2). Some Holocene Indonesian volcanoes, however, are situated above sections of the slab deeper than 150 km (Fig. 1). These ‘spatially anomalous’ arc volcanoes (e.g., Muriah, Ungaran, and Batu Tara) are commonly

* Corresponding author.

E-mail address: jack.ward1@uq.net.au (J.F. Ward).

alkaline in composition and record geochemical characteristics (including suppressed negative Nb-Ta anomalies and negative-to-absent Ba, Pb, and Sr anomalies; Fig. 2) trending towards those of ocean island basalts (OIB; Clapworth, 1989; Edwards et al., 1991; Kirchenbaur et al., 2022; Stoltz et al., 1988; Van Bergen et al., 1992). The Holocene volcanoes Tambora and Sangeang Api, in contrast, are located above ‘normal’ sections of slab (90–150 km depth) but are nevertheless defined by ‘anomalous’ alkaline compositions (e.g., Cooke, 2017; Foden, 1986; Turner et al., 2003). Tambora and the sub-alkaline volcanoes Rinjani and Toba also constitute a geochemically diverse group of Indonesian volcanoes notable for producing extremely violent Quaternary eruptions (volcanic explosivity index [VEI] values ≥ 7 ; Newhall et al., 2018). It is difficult to reconcile the anomalous spatial, geochemical, and eruptive features of these volcanoes with typical subduction processes, suggesting that mechanisms other than subduction-driven mantle metasomatism have contributed to their formation.

Slab segmentation (a generic term describing a variety of processes associated with the development of physical slab discontinuities, including slab tearing) induces complexities in the surrounding mantle and can connect convecting sub-slab mantle with the overlying mantle wedge, trigger mantle melting, and/or generate alkaline volcanic rocks in subduction zone settings (Menant et al., 2016). Slab segmentation via slab tearing has been proposed to generate anomalous arc volcanism, for example, in the Andes (Rosenbaum et al., 2021), Italy (Rosenbaum et al., 2008), New Zealand (McLeod et al., 2022), and the Okinawa Trough (Lin et al., 2004). Slab tearing has also been invoked to explain the formation of some Quaternary Indonesian volcanoes (e.g., Cooke, 2017; Hall and Spakman, 2015; Kirchenbaur et al., 2022; Liu et al., 2021; Yu et al., 2022) and giant porphyry Cu deposits (Fiorentini and Garwin, 2010; Garwin et al., 2005). However, the presence of Indonesian slab tears remains speculative because previous studies were relatively local in scale or supported by lower-resolution datasets. Detailed integration of geophysical and geochemical data relevant to all Holocene Indonesian volcanoes is needed to assess potential links between the origin of

anomalous volcanoes, the formation of giant porphyry ore deposits (Tumpangpitu, Batu Hijau, Elang, and Onto; Fig. 1), and slab segmentation.

In this paper, we test the hypothesis that slab segmentation is a significant causative feature in the generation of anomalous Holocene arc volcanism and giant Pliocene–recent porphyry Cu deposits in Indonesia. To do so, we first use a variety of geophysical datasets to evaluate the geometry of subducted slabs. We then analyse a compilation of geochemical data from Holocene volcanoes to identify geochemical anomalous and evaluate source components and melting mechanisms. Finally, we compare our findings with constraints from numerical models of subduction-driven mantle flow (Burkett and Billen, 2010; Menant et al., 2016). We propose geodynamic mechanisms responsible for the formation of the anomalous volcanoes and porphyry ore deposits, and we also identify other arcs where similar processes may occur.

2. Geological setting

Holocene volcanism and Pliocene–recent porphyry ore deposits in the Sunda arc are associated with the subduction of the Indo-Australian plate below the Sunda plate (Fig. 1). The age of subducting Indo-Australian lithosphere varies significantly along strike, ranging from ~50 Ma at the Sunda Trench to ~150 Ma near Sumbawa (e.g., Seton et al., 2020; Fig. S1). In the Andaman Trench, the Indo-Australian plate moves northward relative to the Sunda plate at ~52 mm/year (Fig. 1), whereas trench-perpendicular subduction in Java occurs at a rate of ~67 mm/yr (DeMets et al., 2010). The trench is retreating at rates of 3.9–24.4 mm/year in the Andaman Trench and advancing along the Sumatran and Javanese sections of the Sunda arc at rates of 12.3–18.4 mm/year (Heuret and Lallemand, 2005). In a number of places along the subduction zone, the subducting oceanic plate contains relatively buoyant crustal material (Fig. 1), including the Ninetyeast Ridge (Sushchevskaya et al., 2016), Investigator Fracture Zone (IFZ; Kopp et al.,

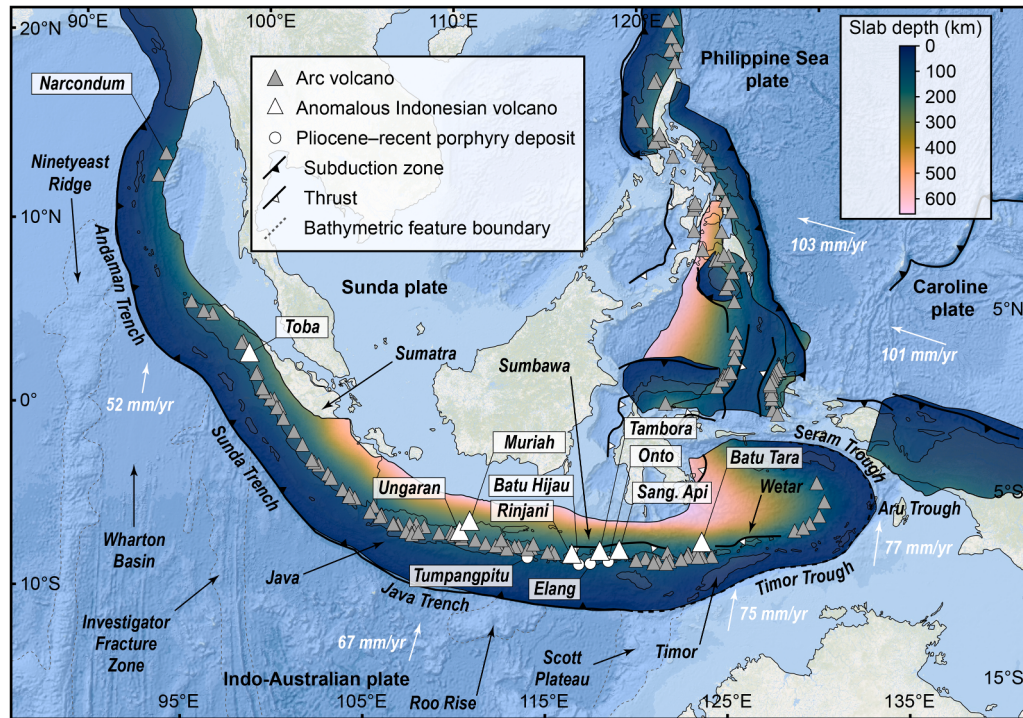


Fig. 1. Map of Southeast Asia showing locations of (1) Holocene arc volcanoes (grey triangles), (2) anomalous Indonesian arc volcanoes (white triangles), (3) giant Pliocene–recent porphyry Cu deposits (white circles), and (4) locations of subducted slabs from the Slab2 model (Hayes et al., 2018). White arrows indicate plate velocities relative to the Sunda plate (DeMets et al., 2010), and the tectonic framework is adapted from Hutchings and Mooney (2021) and Bird (2003).

2008), Roo Rise (Planert et al., 2010), and Scott Plateau (Ely and Sandiford, 2010). The thickness of the overriding plate varies from approximately 18 to 35 km in the Sunda arc (Li and Wang, 2016) and switches from a dominantly continental nature in Sumatra to a dominantly oceanic nature east of Java (Planert et al., 2010).

The Timor Trough denotes the transition from Indo-Australian oceanic lithosphere subduction to the collision of the Banda arc with the Australian passive continental margin (e.g., Harris et al., 2020; Miller et al., 2021; Zhang et al., 2022), which, relative to the Sunda plate, migrates approximately northward at rates of 75–77 mm/year (Fig. 1; DeMets et al., 2010). Ongoing convergence between Indo-Australian continental lithosphere and the Banda arc has generated an inner volcanic arc enclosed by a series of non-volcanic uplifted islands, as well as a ~500 km long volcanic gap (between ~124 and 128.5°E; Fig. 1; Miller et al., 2021). Pb isotope compositions of Neogene–Quaternary igneous rocks located in the inner arc of this now amagmatic zone indicate contributions of subducted Australian continental crust (Elburg et al., 2005), which is supported by recent geophysical studies that image Australian continental lithosphere at depth below the Banda arc (Harris et al., 2020; Zhang et al., 2022).

Indonesian porphyry Cu deposits are concentrated mainly in Java and Sumbawa. Their formation ages are late Oligocene–early Miocene, middle–late Miocene, and Pliocene–recent (Garwin et al., 2005; Maryono et al., 2018). The youngest porphyry Cu deposits are the most fertile and include the giant deposits (i.e., >2 Mt contained Cu; Singer, 1995) Tumpangpitu (4.89–4.03 Ma), Batu Hijau (3.55–3.52 Ma), Elang (2.51–2.38 Ma), and Onto (<0.688 Ma; Burrows et al., 2020; Harrison et al., 2018; Maryono et al., 2018).

3. Results

3.1. Indonesian slab architecture

We used four geophysical datasets to evaluate Indonesian slab architecture. The first is the Slab2 global slab geometry model (Hayes et al., 2018). From the Slab2 model, we also extracted slab depth and dip below each Holocene volcano. To evaluate along-trench variations of slab depth and dip, we projected the Holocene volcanoes to the plate boundary of Bird (2003) and calculated geodesics (the shortest path between two points on the WGS84 ellipsoid) between each volcano. Along-trench distance is the cumulative sum of the geodesics, using Narcondum (Fig. 1) as the origin. The second geophysical dataset, the UU-P07 seismic tomography model (Amaru, 2007; Hall and Spakman,

2015), is a high-resolution P-wave model that accurately resolves slab geometry and mantle structure in Southeast Asia (Hall and Spakman, 2015). To further constrain slab geometry, we integrated the earthquake catalogue of Jiang et al. (2022), which provides a high-resolution record of seismic activity in the Banda arc and eastern Sunda arc, with relocated events from the ISC-EHB Bulletin (which covers the rest of our study area; Engdahl et al., 2020).

The Slab2 model shows continuous subduction of the Indo-Australian plate in Indonesia (Fig. 1). Along the Andaman Trench and north-western section of the Sunda Trench, the Indo-Australian slab reaches a maximum depth of 300 km. Farther east, the Indo-Australian slab subducts to the mantle transition zone, reaching depths of 640 km along the Sunda–Java trench and 660 km in the Banda arc.

Based on the Slab2 model, there is significant along-trench variation of depth to slab (h) in the Sunda and Banda arcs (Fig. 3). The computed h values follow a sinusoidal trend, displaying two segments of eastward-shallowing h bounded by excursions to greater slab depth. In the western part of the Indonesian volcanic arc, h deepens from 88 km to 143 km

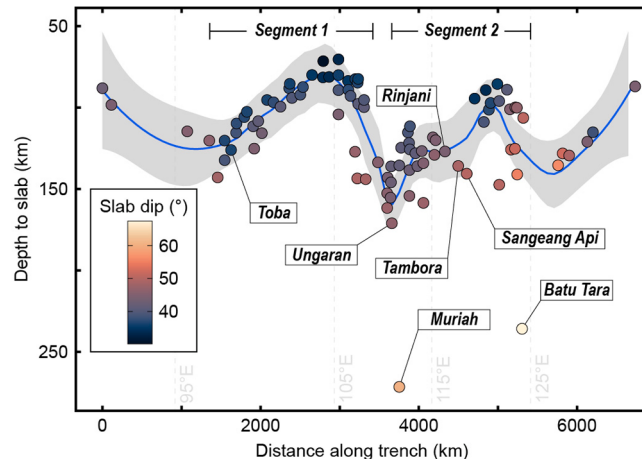


Fig. 3. Projected along-trench distance vs. depth-to-slab (h) for Holocene volcanoes in the Sunda and Banda arcs. The blue curve represents the local polynomial regression line, and the grey shading is the 95% confidence interval. Longitude references (vertical grey lines) were calculated by first interpolating the latitude of hypothetical Indonesian arc volcanoes located at 95°E, 105°E, 115°E, and 125°E. The along-trench distances of these hypothetical arc volcanoes were then calculated.

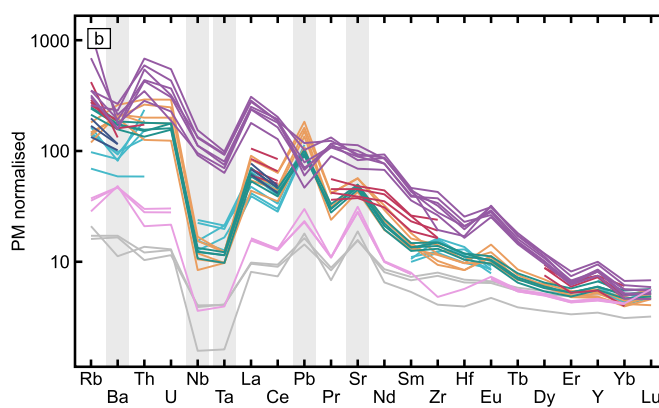
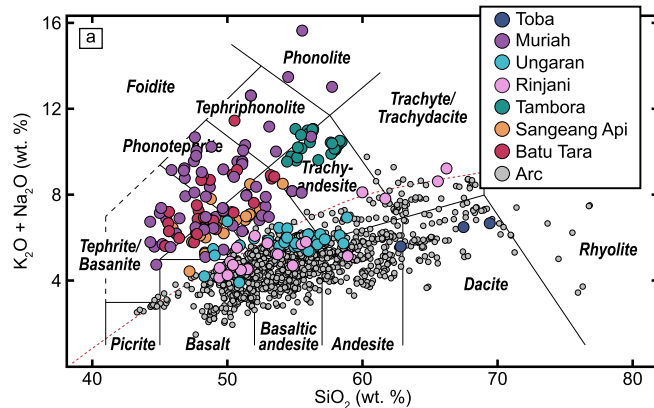


Fig. 2. (a) TAS diagram for Holocene Indonesian volcanoes, and (b) primitive-mantle-normalised multielement diagram of representative samples from anomalous and normal arc volcanoes. Toba data are from Chesner and Rose (1991). Muriah data are from Nicholls and Whitford (1983), Edwards et al. (1991), Kirchenbaur et al. (2022), and Yu et al. (2022). Batu Tara data are from Stoltz et al. (1988) and Van Bergen et al. (1992). Rinjani data are from Foden (1983) and Kirchenbaur et al. (2022). Tambora and Sangeang Api data are from Foden (1986), Turner and Foden (2001), Turner et al. (2003), Gertisser et al. (2012), Cooke (2017), and Suhendro et al. (2021). Representative arc volcano analyses shown in the multielement diagram are from Salak and Guntur (Yu et al., 2022). Data sources for the compilation of arc volcanoes are presented in Supplementary File 1.

at 1457 km along the trench (corresponding to $\sim 97^\circ\text{E}$, the ‘Sumatra excursion’), before shallowing to 70 km at an along-trench distance of 2984 km. Between the along-trench distances of 2984 and 3752 km, h rapidly deepens, reaching a maximum depth of 272 km at Muriah (located at $\sim 111^\circ\text{E}$, the ‘Java excursion’). The westernmost portion of the second arc segment (along-trench distance of 3752–3956 km) is defined by rapid shallowing of h . Depth to slab continues to decrease from 3956 to 4993 km along the trench, but at a more gradual rate. Between 4993 and 5304 km along the trench, h rapidly deepens towards a maximum of ~ 236 km at Batu Tara (located at $\sim 124^\circ\text{E}$, the ‘Sunda–Banda transition excursion’). No Holocene volcanoes are located between along-trench distances of 5319 and 5760 km. East of the volcanic gap, h values range from 87 to 135 km. Slab dip below Muriah and

Batu Tara ($60\text{--}67^\circ$) is greater than below the rest of the arc volcanoes ($41.89^\circ \pm 5.35^\circ$; mean \pm standard deviation), signalling increased slab dip with distance from the trench.

In horizontal depth slices of the UU-P07 tomography model (Fig. 4), the Indo-Australian slab is represented by a positive velocity anomaly subducted below the Sunda and Banda arcs. At a depth of 135 km (Fig. 4a), the Indo-Australian slab tomography anomaly is continuous, curvilinear, and coincides with abundant seismic events (recording magnitudes >4) at depths of 135 ± 50 km in all parts of Indonesia, except between 124°E and 127°E , where such seismic activity is less common. In comparison with the apparently simple geometry of the shallow Indo-Australian slab, horizontal depth slices of the UU-P07 tomography model imply that deeper parts of the slab are deformed. The

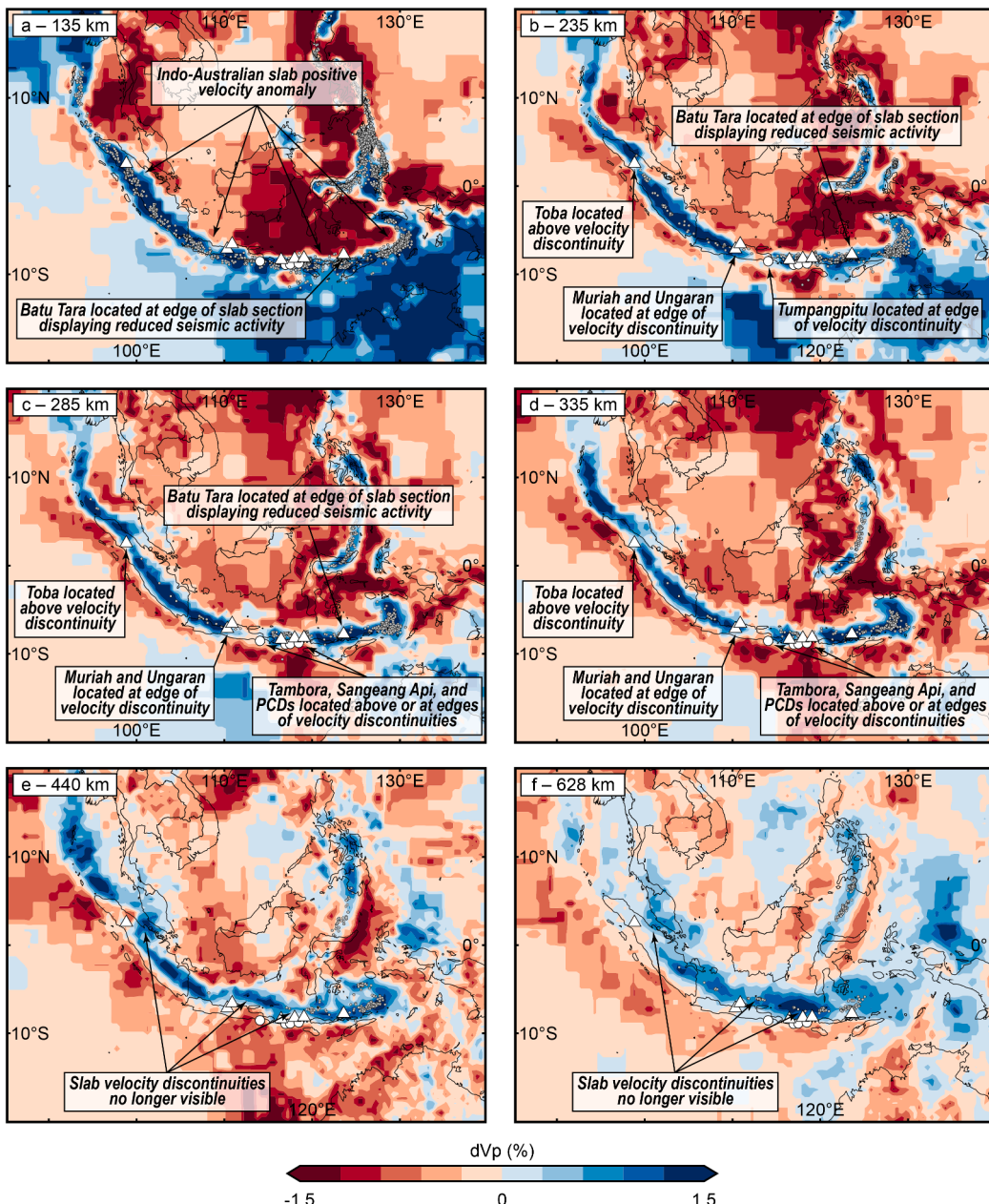


Fig. 4. Horizontal depth slices of the UU-P07 P-wave tomography model (Amaru, 2007; Hall and Spakman, 2015) at depths of (a) 135 km, (b) 235 km, (c) 285 km, (d) 335 km, (e) 440 km, and (f) 628 km. Grey circles represent earthquakes with magnitudes >4 included in the Jiang et al. (2022) catalogue and ISC-EHB Bulletin dataset (Engdahl et al., 2020) within 50 km of the depth slice depth (i.e., the 135 km depth slice displays earthquakes at depths of 85–185 km). White triangles represent the anomalous volcanoes.

Table 1

Summary of volcanoes included in the filtered geochemical data set.

Longitude interval	All volcanoes in interval	Volcanoes included in filtered data set
92–94°E	Barren Island	Barren Island
94–96°E	Narcondum, Seulawah Agam	
96–98°E	Peuet Sague, Burni Telong	
98–100°E	Sinabung, Singkut, Toba, Lubukraya, Sibualbauli, Sorikmarapi, Malintang, Talakmau	
100–102°E	Sarik-Gajah, Tandikat-Singgalang, Marapi, Talang, Kerinci, Sumbing	Marapi
102–104°E	Hululais, Bukit Daun, Kaba Dempo, Patah, Ranau	
104–106°E	Suoh, Sekincau Belirang, Hulubelu, Krakatau, Rajabasa, Pulosari	Krakatau
106–108°E	Karang, Perbakti-Gagak, Salak, Gede, Patuhu, Tangkuban Parahu, Kendang, Papandayan, Guntur, Tampomas	Salak, Gede, Tangkuban Paraju, Guntur
108–110°E	Galunggung, Talagabodas, Ciremai, Slamet, Dieng, Sundoro	Galunggung, Slamet, Sundoro
110–112°E	Sumbing, Ungaran, Telomoyo, Merbabu, Merapi, Muriah, Lawu, Wilis	Ungaran, Merbabu, Merapi, Muriah
112–114°E	Kelud, Kawi-Butak, Arjuno-Welirang, Penanggungan, Semeru, Tengger Caldera, Lamongan, Iyang-Argapura	Tengger Caldera, Lamongan, Iyang-Argapura
114–116°E	Raung, Ijen, Baluran, Buyan-Bratan, Batur, Agung	Ijen, Baluran, Batur
116–118°E	Rinjani, Tambora	Rinjani
118–120°E	Sangeang Api, Wai Sano	Sangeang Api
120–122°E	Ranakah, Inierie, Inielika, Ebulobo, Iya, Paluweh, Kelimutu	Inierie, Iya
122–124°E	Egon, Lewotobi, Leroboleng, Illoboleng, Ililabalekan, Lewotolok, Iliwerung, Batu Tara	Illoboleng, Lewotolok, Iliwerung, Batu Tara
124–126°E	Sirung	
128–130°E	Wurlali, Teon, Nila, Banda Api, Serua, Manuk	Nila

235 km depth slice (Fig. 4b), for example, shows that the Indo-Australian slab velocity anomaly is disrupted, with slab discontinuities (i.e., negative velocity anomalies ‘breaking’ the continuity of the positive slab velocity anomaly) occurring at ~98°E (where slab strike abruptly changes from ~300° to ~330°) and ~110–115°E. Also present in the 235 km depth slice is the interval of reduced seismic activity between 124°E and 127°E. A depth slice at 285 km (Fig. 4c) shows a broadly similar slab geometry to the 235 km depth slice, displaying the 124–127°E section of reduced seismicity and slab tomography discontinuities at ~98°E and 110–115°E. A third tomography discontinuity, approximately located between 118°E and 120°E, also appears in the 285 km depth slice, and all three discontinuities are visible in the 335 km depth slice (Fig. 4d). These tomographic discontinuities are absent in depth slices of mantle transition zone depths (Fig. 4e–f). The 440 km and 628 km depth slices, however, highlight the broadening of the Indo-Australian slab anomaly in the Banda arc. The UU-P07 depth slices and seismic data also reinforce the spatial relationships between the locations of anomalous volcanoes and areas of mantle geophysical anomalism: (1) Toba is located above the ~98°E tomographic discontinuity, which corresponds to the Sumatra excursion (collectively referred to as the ‘Sumatra geophysical anomaly’), (2) Muriah and Ungaran are located at the western edge of the 110–115°E tomographic discontinuity, which corresponds to the Java excursion (collectively referred to as the ‘Java geophysical anomaly’), (3) Rinjani, Tambora, and Sangeang Api are located at the 118–120°E tomographic discontinuity margins (referred to as the ‘Sumbawa geophysical anomaly’), and (4) Batu Tara flanks the western edge of the 124–127°E seismic gap, which corresponds to the Sunda–Banda transition excursion (collectively referred to as the ‘Sunda–Banda transition geophysical anomaly’). Tumpangpitu, Batu Hijau, Elang, and Onto are positioned along the edges of the Java and Sumbawa geophysical anomalies (Fig. 4b–d).

3.2. Geochemistry of Indonesian Holocene volcanoes

To investigate the influence of slab segmentation on the chemistry of Indonesian volcanism, we conducted a comprehensive literature compilation of geochemical data from the anomalous volcanoes. We also carefully curated GEOROC geochemical datasets (Lehnert et al., 2000) from ‘normal’ Sunda and Banda arc volcanoes. To minimise the effects of magma differentiation and crystal accumulation, only samples with $\text{SiO}_2 < 52$ wt.% were included in our analysis. We then divided the filtered geochemical data into 2° longitudinal intervals (volcanoes contained in each interval are displayed in Table 1) and evaluated geochemical indices that track source compositions and melting mechanisms. Alkaline magmas arise from low degree partial melting of metasomatised

mantle (Foley, 1992). Rare earth element ratios (e.g., La/Yb and Tb/Yb) can be used to qualitatively assess depth of melting because heavy rare earth elements like Yb partition strongly in garnet, which is stable at depths >80 km (Lee and Tang, 2020; Moyen, 2009). Ratios of fluid-mobile to fluid-immobile trace elements (e.g., Ba/La and Sr/Nd; Vigouroux et al., 2012; Yang et al., 2018) trace fluids released from subducted altered oceanic crust, and La/Sm ratios are useful for identifying contributions of sediments to arc basalts (Labanieh et al., 2012). High Sr/Y values have been interpreted to represent slab melting, but these geochemical signatures can also be imparted by (1) partial melting of garnet- and amphibole-rich mantle sources, and (2) deep crystallisation of garnet and amphibole (which fractionate Y) and suppression of Sr-fractionating plagioclase (Barber et al., 2021; Chiaradia, 2015; Gomez-Tuena et al., 2007; Lee and Tang, 2020). Finally, fractionated Nb/Y in mafic volcanics reflects mantle metasomatism via slab melts (i.e., melt-induced metasomatism; Hoffer et al., 2008).

Boxplots of filtered geochemical data are reported in Fig. 5. Along-arc compositions of total alkalis (Fig. 5a) are punctuated by excursions to greater values in the 110–112°E (Central Java), 118–120°E (Sumbawa), and 122–124°E (Sunda–Banda transition) intervals, which coincide with the Java, Sumbawa, and Sunda–Banda transition geophysical anomalies, respectively. The alkaline volcanoes from these intervals (Muriah, Ungaran, Sangeang Api, and Batu Tara) are also outstanding for recording significantly higher La/Yb (Fig. 5b) and Tb/Yb (Fig. 5c) values than other primitive samples (including those of ‘normal’ volcanoes within their respective intervals). Median Ba/La values are lowest in the 112°E interval (due to Muriah and Ungaran) and increase eastwards. The 112°E interval also records the lowest median Sr/Nd value (18.1; Fig. 5e), and the Sr/Nd values <20 of Batu Tara drive the 124°E interval Sr/Nd median to a significantly lower value than those of adjacent intervals. Rinjani, in comparison, displays appreciably higher Sr/Nd values (>40) than neighbouring volcanoes. Compiled La/Sm (Fig. 5f) and Sr/Y (Fig. 5g) from Muriah, Ungaran, Sangeang Api, and Batu Tara are elevated relative to the rest of the arc lavas. Median Nb/Y values are <0.5 for all but the 112°E interval (Fig. 5h), in which Muriah records Nb/Y as high as 3.87. Overall, the geochemical data show that primitive samples from Muriah and Ungaran (Central Java), Sangeang Api (Sumbawa), and Batu Tara (Sunda–Banda transition) are geochemically anomalous in most of the considered indices. Herein, we refer to these anomalies as the ‘Java geochemical anomaly’, ‘Sumbawa geochemical anomaly’, and ‘Sunda–Banda transition geochemical anomaly’, respectively.

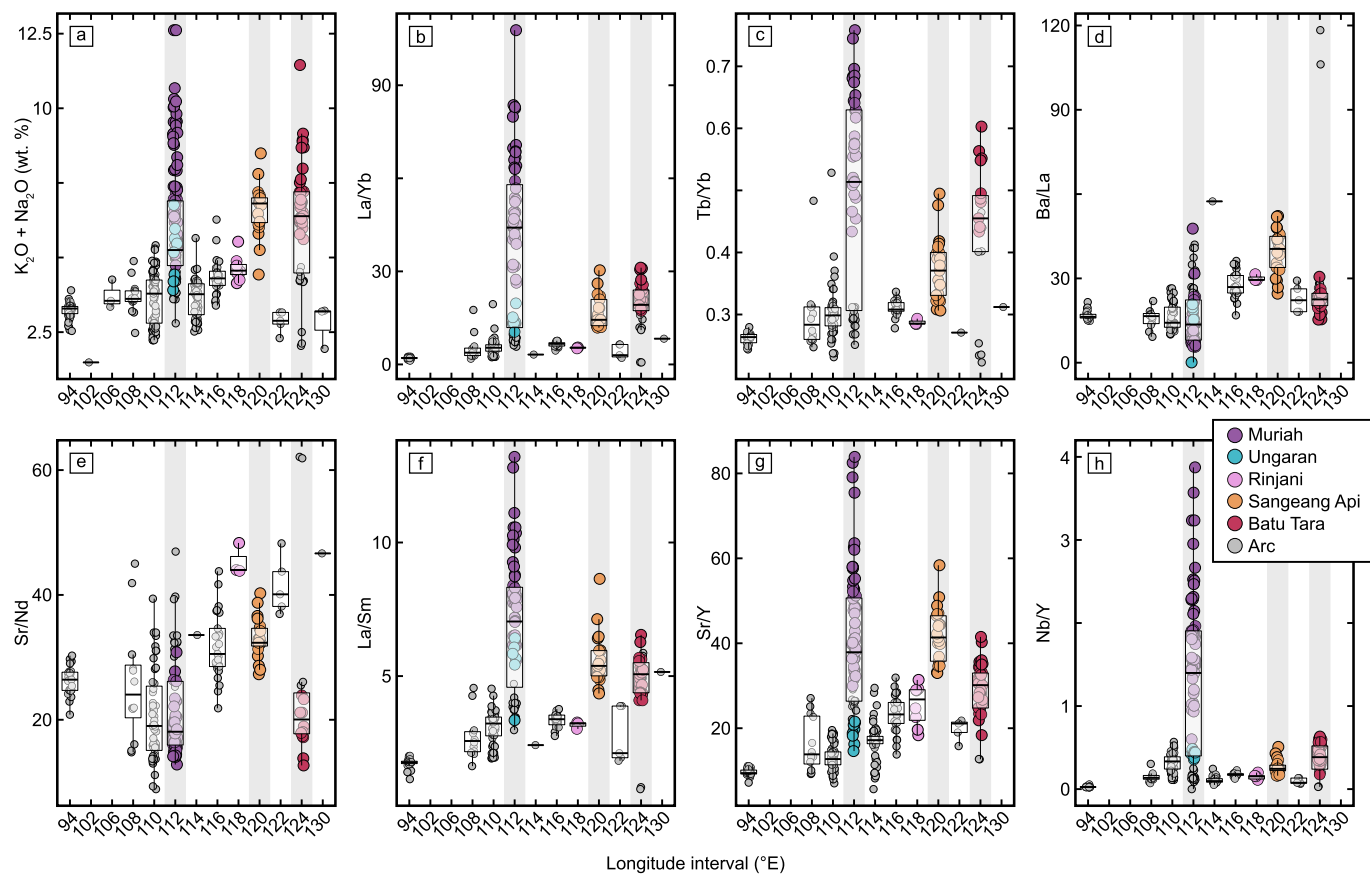


Fig. 5. Along-arc variations of key geochemical indices from filtered samples in the Sunda and Banda arcs. The 112°E, 120°E, and 124°E intervals (shaded grey) coincide with the Java, Sumbawa, and Sunda–Banda transition geochemical anomalies, respectively. Volcanoes included in each longitudinal interval are displayed in Table 1. Note that the maximum longitude of each interval is reported on the x axis (i.e., the 110–112°E interval is denoted as '112').

4. Discussion

4.1. The role of slab segmentation in the genesis of anomalous Indonesian volcanism

Geophysical anomalies in the Indo-Australian slab are recognised below northern Sumatra (~98°E), Central Java (110–115°E), Sumbawa (118–120°E), and the Sunda–Banda transition (124–127°E; Figs. 3–4). All geophysical anomalies, except of northern Sumatra, coincide with geochemical anomalies recognised in our filtered dataset (Fig. 5). The spatial correlation between mantle geophysical and geochemical anomalies suggests that they could be products of slab deformation (including slab tearing) and anomalous melt generation. A genetic link between areas of geochemical and geophysical anomalism is supported by the subduction of buoyant features in the Sunda and Banda arcs (Fig. 1). The location of the Sumatra geophysical anomaly, for example, corresponds to the intersection between the IFZ and the Sunda Trench (Fig. 1). At the Java Trench, the buoyant Roo Rise is being subducted, and the down-dip projection of the Scott Plateau is located at the western edge of the Sunda–Banda transition anomaly (Fig. 1). Arrival of buoyant bathymetric features, such as seamounts and aseismic ridges, at convergent margins can impede local subduction regimes and initiate tearing of the subducting slab (Rosenbaum and Mo, 2011). Subduction of fracture zones can also generate slab tears because rheological contrasts allow sections of slab adjacent to these weak structures to move independently (Burkett and Billen, 2010). In turn, slab tearing may generate poloidal asthenospheric flow capable of triggering mantle melting (Menant et al., 2016). The geochemical expression of volcanism related to slab tearing, therefore, generally includes trace element

characteristics intermediate between those of arc and alkaline OIB lavas (Rosenbaum et al., 2021, 2008).

In the case of the Sumatra geophysical anomaly, the IFZ marks the transition from subduction of relatively young, warm, and buoyant lithosphere of the Wharton Basin (Figs. 1 and S1) to the denser and less buoyant Cretaceous–Jurassic lithosphere that subducts elsewhere along the Sunda arc (Jacob et al., 2014; Liu et al., 2021). The seismic expression of the subducted portion of the IFZ extends to a depth of ~200 km beneath Toba (Koulakov et al., 2016). Northward continuation of the IFZ is supported by reconstructions of subducted magnetic isochrons (Jacob et al., 2014). Based on interpretations of seismic tomography models, a slab tear caused by subduction of the IFZ has been proposed to be located below Toba (Hall and Spakman, 2015; Koulakov et al., 2016; Liu et al., 2021). Observations of the highly contorted and segmented slab from seismic tomography presented here (Fig. 4), as well as excursions to deeper h (Fig. 3), are consistent with the presence of a sub-vertical tear beneath Toba (Fig. 6). Although no Holocene samples from the calc-alkaline Toba meet the requirements of our geochemical filter, and we are thus unable to directly comment on the geochemical relationship between Toba and the postulated slab tear, we note that tear-derived thermal upwellings have been invoked to explain isotopically-enriched Quaternary Toba lavas (via melting of rising diapirs of Nicobar fan sediments; Gao et al., 2022), as well as increased magma generation and volatile delivery to the Sumatran mantle wedge, triggering the extremely explosive eruptions at Toba (Koulakov et al., 2016).

The Java and Sumbawa geochemical anomalies correspond to areas of slab segmentation inferred from the geophysical data. In seismic tomography depth slices (Fig. 4), the Java geophysical anomaly is

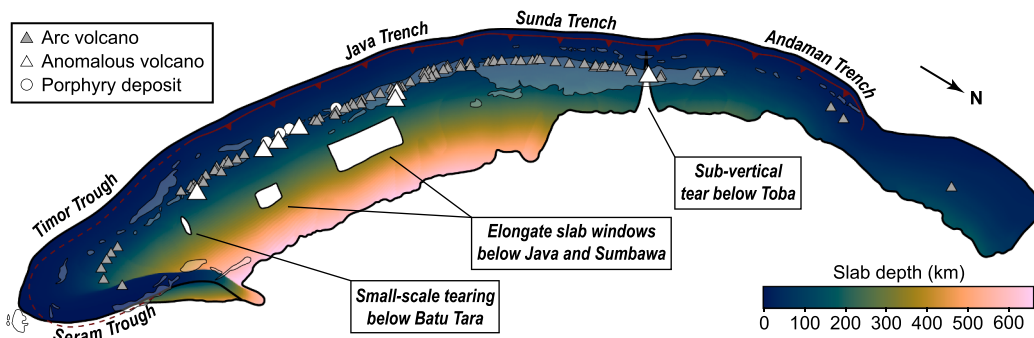


Fig. 6. Schematic three-dimensional model of slab geometry in Indonesia (based on the Slab2 model) highlighting proposed spatial relationships between slab tearing, anomalous volcanoes, and porphyry ore deposits.

expressed as an elongate low velocity anomaly present between approximately 110°E and 115°E at depths of 185–400 km, which overlaps with an excursion to deeper h (Fig. 3). The tomographic expression of the Sumbawa geophysical anomaly is located at 235–400 km depth between approximately 118°E and 120°E (Fig. 4). Unlike the Java geophysical anomaly, however, the Sumbawa geophysical anomaly is not associated with any h excursions (Fig. 3). Primitive Holocene lavas from Muriah (Java geochemical anomaly) and Sangeang Api (Sumbawa geochemical anomaly) are alkaline (Figs. 2 and 5a; they are also potassic), LREE-enriched (Fig. 5b), and record $Tb/Yb > 0.4$ (Fig. 5c), collectively representing low degree partial melting of enriched mantle in the garnet stability field. The mean Ba/La value of Muriah lavas (12.2) is MORB-like (<15; Yang et al., 2018), and Sr/Nd (Fig. 5e) values recorded by Muriah overlap with those of hypothetical dry mantle melts ($Sr/Nd < 20$) modelled by Vigouroux et al. (2012). These characteristics, together with negative-to-absent Sr and Pb anomalies (Fig. 2), are implicit of reduced slab fluid contributions. Although few data are available, Ungaran displays elevated La/Yb and decreased Ba/La (albeit with a positive Pb anomaly; Fig. 2). Slab fluid proxies of Sangeang Api, however, overlap with ‘typical’ subduction values. Median La/Sm values >5 (Fig. 5f) signal increased sediment contributions to anomalous Java and Sumbawa lavas, which were likely delivered as sediment melts (Edwards et al., 1991; Handley et al., 2011; Kirchenbaur et al., 2022; Turner and Foden, 2001; Vigouroux et al., 2012). Muriah and Sangeang Api lavas have $Sr/Y > 40$ (Fig. 5g), which is commonly interpreted as a slab melt signature (‘adakites’; e.g., Castillo, 2012). Adakites, however, typically have $SiO_2 > 60$ wt%, and enigmatic ‘low silica adakites’ are characterised by $Na_2O > 4.1$ wt%, $Sr > 2051$ ppm, $Ni > 103$ ppm, and $Sr/Y > 162$ (Castillo, 2012). These geochemical features are not displayed by primitive samples from Muriah and Sangeang Api, which have mean values of 3.34 and 3.78 wt% Na_2O , 1514 and 1010 ppm Sr , 42 and 17 ppm Ni , and 48 and 42 Sr/Y , respectively. Nevertheless, a slab melt component is necessary to explain the super-chondritic Nb/Ta values and HFSE concentrations (Fig. 2; Kirchenbaur et al., 2022), as well as $Nb/Y > 1$ (Fig. 5h) and covariations of $^{206}Pb/^{204}Pb$ and $\delta^{98/95}Mo$ (Yu et al., 2022), in Muriah rocks. In contrast, elevated Sangeang Api Sr/Y values may arise from the melting of garnet-bearing asthenosphere (consistent with previous trace element modelling; Turner et al., 2003) and/or deep fractionation of amphibole (consistent with cumulate amphibole in Sangeang Api xenoliths; Cooke, 2017). The Holocene volcanic rocks of Tambora (located at 8.25°S 118°E) are too evolved to be included in our geochemical analysis, but this volcano erupts shoshonites with enriched trace element compositions akin to those of the other anomalous volcanoes (Fig. 2; Gertisser et al., 2012; Turner et al., 2003; Vigouroux et al., 2012). Trace element characteristics of shoshonitic, olivine-hosted melt inclusions demonstrate that the slab contribution in Tambora is dominated by sediment flux (rather than slab fluids), indicating elevated slab surface temperatures (Vigouroux et al., 2012).

Overall, the geochemical data from the Java and Sumbawa anomalies suggest deep, low degree partial melting of enriched mantle with enhanced contributions of sediment melt. However, the subducted Indo-Australian slab is one of the oldest and coldest slabs on Earth (Syracuse et al., 2010); therefore, low slab surface temperatures would favour the addition of slab fluids over sediment melts to the mantle wedge (Ruscitto et al., 2012). Based on these geochemical constraints, as well as the presence of slab velocity discontinuities and excursions to deeper h , we suggest that elongate slab tears (akin to slab ‘windows’) exist below Java and Sumbawa (Fig. 6). Consistent with numerical modelling of mantle flow induced by slab tearing (Menant et al., 2016), we postulate that these tears have produced poloidal asthenospheric flow that has raised temperatures, generating deep, low degree partial melting of enriched mantle sources. Although the anomalous Java and Sumbawa volcanoes share many petrographic and geochemical characteristics, Sumbawa lavas lack evidence for slab melting and display stronger fluid components. These disparities could be due to Muriah (the most geochemically anomalous volcano of the Java anomaly) being located above a comparatively younger, deeper, and possibly dehydrated section of slab with a considerably larger tear, which may enable slab melting. Furthermore, although the buoyant Roo Rise is undergoing subduction at the Java Trench, there is no evidence for slab tearing at depths <185 km in Java and Sumbawa. If a constant subduction rate of 6.7 cm/year (DeMets et al., 2010) and depth of ~400 km for the bottom of the tears (based on the geophysical analysis presented here) are assumed, a simple calculation suggests that the buoyant feature responsible for slab segmentation arrived at the trench at ~6 Ma. Although the modern Roo Rise subduction may indeed generate slab tearing, time-space relationships indicate slab segmentation in Sumbawa and Java was likely initiated by older bathymetric structures (Hall and Spakman, 2015).

Unlike the other anomalous volcanoes, Batu Tara (Sunda-Banda transition) is not positioned at the edge of a negative velocity anomaly (Fig. 3), and no slab tears are resolved in the vicinity of Batu Tara by higher resolution (but spatially restricted) tomography models (e.g., Harris et al., 2020; Wehner et al., 2022). Earlier studies of relocated hypocentres (e.g., Ely and Sandiford, 2010 and references therein) recognised an absence of intermediate-depth earthquakes (depths of 70–300 km) between ~124°E and 128°E, referred to as the ‘Wetar Seismic Gap’. This seismic gap is also represented by the ISC-EHB Bulletin data evaluated in this study (Fig. S2). Batu Tara is located at the western edge of the Wetar Seismic Gap (Fig. 3), which has been interpreted as a slab window and/or actively rupturing section of the Indo-Australian slab (Ely and Sandiford, 2010; Sandiford, 2008). However, a continuous slab in the Wetar Seismic Gap (which contains subducted continental lithosphere) is resolved by the high-resolution seismic tomography model of Harris et al. (2020). Furthermore, the detailed seismic catalogue of Jiang et al. (2022) records intermediate-depth seismic events in the Wetar Seismic Gap, albeit less frequently (and with smaller magnitudes) than elsewhere in the Sunda

and Banda arcs (Fig. 3 and S2). Rather than a regional-scale slab window (like those proposed below Java and Sumbawa in this study), it is possible that the Wetar Seismic Gap is associated with subduction termination following arc–continent collision (Harris et al., 2020). Nevertheless, back-arc thrusting precludes volcanism due to lithospheric extension, no plumes are detectable in seismic tomography (Fig. 3), and Batu Tara geochemical compositions (characterised by extreme enrichments of alkali elements and elevated La/Yb and Sr/Y; Fig. 4) require deep melting of an enriched source. Decreased slab fluid contributions implied by Batu Tara Sr/Nd systematics (Fig. 5) are supported by U- and Ra-series isotope data (Hoogewerff et al., 1997; Turner and Foden, 2001). Batu Tara is positioned ~236 km above the Indo-Australian slab (in an isolated position ~80 km behind the arc; Fig. 1), and $^{206}\text{Pb}/^{204}\text{Pb}$ values (19.02 ± 0.3) are consistent with melting of subducted Australian continental lithosphere, which has also been identified in the sources of Quaternary Indonesian arc volcanoes east of ~122°E (Elburg et al., 2005, 2004; Zhang et al., 2022). Given these geochemical and geophysical properties, the origin of Batu Tara is difficult to explain without invoking some form of geodynamic process associated with the subducted Indo-Australian slab. One possible means of generating far-field subduction-related volcanism is mantle convection above edges of slabs in the mantle transition zone (e.g. Ward et al., 2021). However, the edge of the Indo-Australian slab is ~200 km north of Batu Tara (Fig. 1), and the slab below Batu Tara is too shallow to trigger such a process. Silica-undersaturated Roman Province lavas (geochemically akin to Batu Tara lavas) have been explained by carbonate assimilation (summarised in Peccerillo and Terre, 2017). Carbonate assimilation at Batu Tara may be unlikely, however, due to the oceanic nature of the overlying plate, mantle-like Batu Tara $\delta^{18}\text{O}$ values (Van Bergen et al., 1992), and Pb isotope evidence for negligible contributions of subducted shelf sediments to collisional Banda arc volcanics (Elburg et al., 2002, 2004, 2005). Batu Tara is positioned above the projected eastern terminus of the buoyant Scott Plateau (Fig. 1), which, based on earthquakes signalling down-dip compression below Flores, has been subducted to depths of ~300 km (Ely and Sandiford, 2010). Considering these observations, we speculate that small-scale slab tearing (i.e., below the resolution of available seismic tomography models) could be responsible for Batu Tara volcanism, but we acknowledge that this is a relatively low-confidence feature.

4.2. Links between slab segmentation and eruption explosivity

Most Indonesian volcanoes have recorded VEIs <5 (Malawani et al., 2021), but Toba, Rinjani, and Tambora have produced Quaternary eruptions with VEIs ≥ 7 (Newhall et al., 2018). Spatial correlations between these volcanoes and proposed slab tears possibly link tearing to anomalously explosive eruptions. Convergence rate, crustal thickness, and local stress regime are the principal parameters governing eruption frequency and size in arcs (De Silva, 2008; Hughes and Mahood, 2008). Of these parameters, convergence rate is considered the most important because faster convergence rates facilitate sustained and voluminous basalt production, ultimately generating greater silicic magma volumes (Hughes and Mahood, 2008). Thick, old continental crust and local extension enable long-term magma storage and increased magmatic differentiation (Hughes and Mahood, 2008). Even where convergence rate, stress regime, and crustal thickness are appropriate for the development of large caldera-forming eruptions, most eruptions record VEIs <6 (De Silva, 2008). More violent eruptions are associated with ‘flare-up’ events, in which increased mantle contributions enhance magmatic flux (De Silva, 2008). Given the modest convergence rates (~52–67 mm/yr; DeMets et al., 2010), thin crust (Li and Wang, 2016), and neutral-to-compressive back-arc strain regimes in Indonesia (Heuret and Lallemand, 2005), we speculate that tear-driven asthenospheric flow could have enhanced mantle magmatic flux, enabling VEI ≥ 7 eruptions. Detailed geochemical and thermomechanical modelling of plumbing system anatomy and dynamics, however, is required to

rigorously assess links between slab tearing and eruption explosivity in Indonesia.

4.3. Slab tearing as a driver for porphyry ore deposit formation

Porphyry Cu deposits are typically associated with oxidised, calc-alkaline magmas, in areas with crust >45 km thick (Lee and Tang, 2020). The lower abundance of porphyry Cu deposits in island arcs and immature continental arcs is purportedly due to the inability of these subduction systems to fractionate garnet, which decreases residual melt Fe concentrations (whilst also oxidising the melt), thereby reducing S solubility (Lee and Tang, 2020). Because the behaviour of Cu, a chalcophile element, in magmatic arcs is inherently controlled by S availability, garnet fractionation also lowers melt Cu concentrations. A corollary of this process is that although deep garnet fractionation depletes melts of Cu, melt oxidation triggers conversion of sulphide to sulphate, which facilitates the mobilisation and scavenging of Cu from the magma during fluid saturation at shallow depths (Lee and Tang, 2020). In areas of thin crust, slab melting (involving residual garnet) has been invoked as an alternative avenue of magma oxidation leading to ore genesis (Lee and Tang, 2020).

The giant Pliocene–recent Indonesian porphyry Cu deposits Tumpangpitu, Batu Hijau, Elang, and Onto are positioned near the margins of the slab tears proposed in this study (Figs. 4 and 6), where the crust is <25 km thick (Li and Wang, 2016). Based on the model of Lee and Tang (2020), the Indonesian crust is too thin to fractionate garnet and generate prospective magmas, which is supported by mean La/Yb <10 and Sr/Y <20 for most of the ‘normal’ arc volcanoes (Fig. 5). Although tear-driven slab melting below Central Java is evidenced by Muriah lavas, there is no indication of recent slab melting from Holocene volcanoes in Eastern Java (where Tumpangpitu is located) and Sumbawa (where Batu Hijau, Elang, and Onto are located). Furthermore, the only Pleistocene volcanoes located in Sumbawa (Sangenges and Soromundi) have erupted highly anomalous, silica-undersaturated lavas (Foden and Varne, 1980), but Nb/Y values <0.3 are inconsistent with slab melting, which yields Nb/Y >0.6 (Rosenbaum et al., 2021). Batu Hijau, Elang, and Onto, therefore, are not only anomalously large, they are also located in a geodynamic setting lacking the crustal structure and mantle melting conditions typically considered necessary for their formation.

Unfortunately, limited geochemical data are available from the deposits, and samples are typically too evolved or altered to thoroughly assess source components. Nonetheless, Batu Hijau is calc-alkaline yet displays juvenile $^{143}\text{Nd}/^{144}\text{Nd}$ compositions, as well as depleted B and Li concentrations in magmatic amphibole that have been ascribed to dehydration of upwelling asthenosphere above a kink or tear in the Indo-Australian slab (Fiorentini and Garwin, 2010). Although our study does not preclude contributions of dehydrating asthenosphere to Batu Hijau (on the contrary, slab tearing is a viable mechanism of delivering juvenile material to the mantle wedge; Menant et al., 2016), we suggest that the existence of this deposit, and indeed the other giant Indonesian porphyry Cu deposits, could be related to tear-driven mantle melting, within the garnet stability field, that generates oxidised melts akin to those formed in thick continental arcs and areas undergoing slab melting (Lee and Tang, 2020). Garnet involvement in Batu Hijau ore genesis is consistent with Sr/Y of ~30–61 from representative samples of least-altered Batu Hijau andesite, diorite, and tonalite (Fiorentini and Garwin, 2010). Primitive samples from the anomalous Pleistocene volcanoes Sangenges and Soromundi also record Sr/Y of 33–80 (Foden and Varne, 1980), possibly signalling melting in the garnet stability field below Sumbawa during Pleistocene time.

Two important aspects of our tear-related model for Tumpangpitu, Batu Hijau, Elang, and Onto require further consideration. First, the relatively older age of the Tumpangpitu deposit (and the absence of other Pliocene–recent porphyry deposits associated with the Java anomaly) implies slab tearing alone is insufficient to generate porphyry ore deposits in island arcs. The present-day Java anomaly is larger than

the Sumbawa anomaly, but geochemical data reflect reduced slab fluid contributions to anomalous Holocene Javanese volcanoes (Figs. 2 and 5). It is well-known that porphyry ore deposits are associated with hydrous melts (Wilkinson, 2013), so it is unlikely that a deposit will form if the melt is insufficiently hydrous, even if a tear facilitates melting in the garnet stability field. Based on a ~6 Ma estimate for the arrival of the buoyant feature and the 4.89–4.03 Ma age of the Tumpangpitu deposit (Harrison et al., 2018), ore formation seems to have taken place during the early stage of tearing. Therefore, the Java anomaly could have generated tear-driven melts within the garnet stability field, yet still be shallow enough to contribute fluid volumes adequate to generate a hydrous melt, as is the case for the anomalous volcanoes associated with the Sumbawa anomaly. Second, host rocks of Tumpangpitu, Batu Hijau, and Onto mineralisation are calc-alkaline, contrasting with the alkaline signatures of the associated anomalous volcanoes. This is not entirely unexpected, given the varied geochemical response of tear-related lavas along the Sunda-Banda arc. In this context, it is apparent that the geochemical response to slab tearing is variable, but some degree of anomalism is consistently displayed by the tear-related magmas. In the case of the Indonesian porphyry deposits, geochemical anomalism is represented by asthenospheric sources and/or garnet signatures. To fully test our hypothesis, future work should focus on detailed characterisation of putative garnet signatures in deposit host rocks.

4.4. The global volcanic and metallogenic expression of slab segmentation

Anomalous volcanism associated with slab tearing has been recognised in other modern arcs, raising the possibility that tear-related volcanism could be characterised by common geochemical signatures. In the Andes, anomalous Holocene volcanoes have been linked to tears in the Nazca slab (Rosenbaum et al., 2021, 2019). These anomalous volcanoes are alkaline and display hybrid arc-OIB trace element characteristics (i.e., enriched incompatible element concentrations with suppressed LILE and HFSE anomalies) reflective of deeper melting, reduced contributions of slab fluids, and enhanced contributions of slab melts (Rosenbaum et al., 2021). In southern Italy, Mt Etna and Mt Vulture lavas are also alkaline and display OIB-like geochemical features, owing to enhanced asthenospheric contributions due to slab tearing (summarised in Rosenbaum et al., 2008).

Within this broader geochemical framework, alkaline and OIB-like signatures are apparently key features of tear-related arc lavas. However, there is appreciable geochemical variation within the geochemically anomalous Indonesian volcanoes: Muriah and Batu Tara (noteworthy for greater incompatible element enrichment, reduced Nb-Ta anomalies and/or negative-to-absent Ba, Pb, and Sr anomalies) fall closer to the ‘OIB’ end of a hypothetical arc-OIB geochemical continuum than, for example, Tambora and Sangeang Api, which retain stronger ‘arc’ signatures (i.e., more pronounced Nb-Ta depletions and positive Pb anomalies; Fig. 2). A similar phenomenon was identified by McLeod et al. (2022), who demonstrated that in the Alexandra Volcanic Group (New Zealand), the petrogenetic influence of slab tearing is proportional to distance from the trench, leading to the eruption of lavas displaying arc, intraplate (in this case, alkaline and OIB-like), and hybrid arc-intraplate compositions. Another point of consideration is that not all tears have led to the eruption of geochemically anomalous lavas. For example, Toba and Rinjani lavas are subalkaline, as are tear-related, high-melt-flux lavas in the Okinawa Trough (Lin et al., 2004). This compositional dichotomy implies that although alkaline and OIB-like compositions may be a common signature of tear-related lavas, such lavas may, in fact, be compositionally diverse. A key consequence of this diversity is that slab tears may be represented in the magmatic record by anomalous melt flux, rather than by geochemical anomalism.

The genetic relationship between slab tearing and metal fertility in Indonesia also implicates slab tearing as a possible ore-forming mechanism in other island arcs. In Papua New Guinea, the Lihir and Kabang porphyry systems are positioned at the periphery of a sub-vertical tear in

the tightly-curved Solomon Sea slab (Holm et al., 2019). In the northern Philippines, the Baguio district and giant Lepanto-Far South East porphyry systems have been linked to a tear formed via subduction of the buoyant Scarborough Ridge (Cooke et al., 2005; Hollings et al., 2011). Although these deposits are associated with alkaline and/or adakitic melts, the exact role of ridge subduction in the genesis of porphyry ore deposits in the Philippines is unclear (Hollings et al., 2011), and the cause of slab tearing (as well as contributions to metal endowment) in Papua New Guinea remains an open question (Holm et al., 2019). Considering the proposed relationships between slab tearing and metallogenesis in Indonesia, the role of slab tearing in forming island arc porphyry systems (where the crust is too thin to induce garnet fractionation and slab melting may be absent) represents an important avenue of future research, especially given the rising demand for metals such as Cu.

5. Conclusion

Our analysis suggests that the anomalous Holocene Indonesian volcanoes are positioned above the edges of tears in the Indo-Australian slab. Below Toba, a sub-vertical slab tear propagates to depths of approximately 400 km. Elongate slab tears are located below Java and Sumbawa (at depths between 185 and 400 km), and a small-scale tear may be located below Batu Tara. Compositions of mafic samples from geochemically anomalous volcanoes reflect variable contributions from deep, enriched mantle sources due to low degree partial melting associated with tear-driven mantle flow. Spatial and temporal links of giant Indonesian porphyry deposits with slab tears and anomalous volcanism suggest slab tearing may have contributed to the formation of these deposits by inducing mantle melting in the garnet stability field, mirroring the effects of magmatism in areas of thick crust or slab melting. We also speculate that slab tearing may enhance mantle melt flux (potentially promoting long-term magma storage and increased magmatic differentiation) leading to extremely violent Quaternary eruptions at Toba, Rinjani, and Tambora.

CRediT authorship contribution statement

Jack F. Ward: Writing – review & editing, Writing – original draft, Methodology, Investigation, Funding acquisition, Formal analysis, Conceptualization. **Gideon Rosenbaum:** Writing – review & editing, Supervision, Project administration, Methodology, Investigation, Funding acquisition, Conceptualization. **Teresa Ubide:** Writing – review & editing, Supervision, Project administration, Methodology, Investigation, Funding acquisition, Conceptualization. **Mike Sandiford:** Writing – review & editing, Supervision, Project administration, Methodology, Investigation, Funding acquisition, Conceptualization.

Declaration of competing interest

The authors declare that they have no known competing financial interests or personal relationships that could have appeared to influence the work reported in this paper.

Data availability

All data are available in the Supplementary Material. Code associated with this article can be found at <https://www.github.com/JackFWard/-Slab-segmentation-anomalous-arc-volcanism-and-giant-porphyry-copper-deposits-in-Indonesia->.

Acknowledgements

This research was funded by an ARC Discovery Grant (DP200101566). Jack Ward acknowledges support from the Australian Government

Research Training Program scholarship awarded by The University of Queensland and the Sandfire Resources Lou Christie Award. Jonny Wu, Derya Gürer, Dan Sandiford, and Chengxin Jiang are thanked for insightful discussion and suggestions. We sincerely appreciate Rosemary Hickey-Vargas for expert editorial handling and two anonymous reviewers, whose detailed, constructive, and insightful comments significantly improved the manuscript.

Supplementary materials

Supplementary material associated with this article can be found, in the online version, at [doi:10.1016/j.epsl.2023.118532](https://doi.org/10.1016/j.epsl.2023.118532).

References

- Amaru, M., 2007. Global Travel Time Tomography With 3-D Reference Models. Utrecht University.
- Barber, N.D., Edmonds, M., Jenner, F., Audébat, A., Williams, H., 2021. Amphibole control on copper systematics in arcs: Insights from the analysis of global datasets. *Geochim. Cosmochim. Acta. Early Access*.
- Bird, P., 2003. An updated digital model of plate boundaries: *Geochemistry, Geophysics, Geosystems* 4 (3).
- Burkett, E.R., Billen, M.I., 2010. Three-dimensionality of slab detachment due to ridge-trench collision: Laterally simultaneous boudinage versus tear propagation: *Geochemistry, Geophysics, Geosystems* 11 (11).
- Burrows, D.R., Rennison, M., Burt, D., Davies, R., 2020. The Onto Cu-Au discovery, eastern Sumbawa, Indonesia: A large, Middle Pleistocene lithocap-hosted high-sulfidation covellite-pyrite porphyry deposit: *Economic Geology* 115 (7), 1385–1412.
- Castillo, P.R., 2012. Adakite petrogenesis: *Lithos*, 134, p. 304–316.
- Chesner, C.A., Rose, W.I., 1991. Stratigraphy of the Toba tuffs and the Evolution of the Toba caldera Complex, 53. *Bulletin of Volcanology*, Sumatra, Indonesia, pp. 343–356.
- Chiarradia, M., 2015. Crustal thickness control on Sr/Y signatures of recent arc magmas: an Earth scale perspective: *Scientific reports* 5 (1), 1–5.
- Claproth, R., 1989. Petrography and Geochemistry of Volcanic Rocks from Ungaran, Central Java, Indonesia.
- Cooke, B., 2017. Petrology and geochemistry of Sangeang Api and recent volcanism in the Sumbawa-Flores sector of the Sunda Arc: the response of along-arc geochemistry to subduction processes.
- Cooke, D.R., Hollings, P., Walshe, J.L., 2005. Giant porphyry deposits: characteristics, distribution, and tectonic controls: *Economic geology* 100 (5), 801–818.
- De Silva, S., 2008. Arc magmatism, calderas, and supervolcanoes: *Geology* 36 (8), 671–672.
- DeMets, C., Gordon, R.G., Argus, D.F., 2010. Geologically current plate motions. *Geophys. J. Int.* 181 (1), 1–80.
- Edwards, C., Menzies, M., Thirlwall, M., 1991. Evidence from Muriah, Indonesia, for the interplay of supra-subduction zone and intraplate processes in the genesis of potassio alkaline magmas. *J. Petrol.* 32 (3), 555–592.
- Elburg, M., Foden, J., Van Bergen, M., Zulkarnain, I., 2005. Australia and Indonesia in collision: geochemical sources of magmatism. *J. Volcanol. Geotherm. Res.* 140 (1–3), 25–47.
- Elburg, M., Van Bergen, M., Foden, J., 2004. Subducted upper and lower continental crust contributes to magmatism in the collision sector of the Sunda-Banda arc. *Indonesia: Geology* 32 (1), 41–44.
- Elburg, M.A., Van Bergen, M., Hoogewerff, J., Foden, J., Vroon, P., Zulkarnain, I., Nasution, A., 2002. Geochemical trends across an arc-continent collision zone: magma sources and slab-wedge transfer processes below the Pantar Strait volcanoes. *Indonesia: Geochimica et Cosmochimica Acta* 66 (15), 2771–2789.
- Ely, K.S., Sandiford, M., 2010. Seismic response to slab rupture and variation in lithospheric structure beneath the Savu Sea, Indonesia: *Tectonophysics* 483 (1–2), 112–124.
- Engdahl, E.R., Di Giacomo, D., Sakarya, B., Gkarlaouni, C.G., Harris, J., Storchak, D.A., 2020. ISC-EHB 1964–2016, an improved data set for studies of Earth structure and global seismicity. *Earth and Space Science* 7 (1), e2019EA000897.
- Fiorentini, M.L., Garwin, S.L., 2010. Evidence of a mantle contribution in the genesis of magmatic rocks from the Neogene Batu Hijau district in the Sunda Arc, South Western Sumbawa, Indonesia: Contributions to Mineralogy and Petrology 159 (6), 819–837.
- Foden, J., 1983. The petrology of the calcalkaline lavas of Rindjani volcano, east Sunda arc: a model for island arc petrogenesis. *J. Petrol.* 24 (1), 98–130.
- Foden, J., 1986. The petrology of Tambora volcano, Indonesia: a model for the 1815 eruption. *J. Volcanol. Geotherm. Res.* 27 (1–2), 1–41.
- Foden, J., Varne, R., 1980. The petrology and tectonic setting of Quaternary—Recent volcanic centres of Lombok and Sumbawa. *Sunda Arc: Chemical Geology* 30 (3), 201–226.
- Foley, S., 1992. Vein-plus-wall-rock melting mechanisms in the lithosphere and the origin of potassio alkaline magmas. *Lithos* 28 (3–6), 435–453.
- Gao, M.H., Liu, P.P., Chung, S.L., Li, Q.L., Wang, B., Tian, W., Li, X.H., Lee, H.Y., 2022. Himalayan zircons resurface in Sumatran arc volcanoes through sediment recycling. *Communications Earth & Environment* 3 (1), 1–11.
- Garwin, S., Hall, R., Watanabe, Y., 2005. Tectonic setting, geology, and gold and copper mineralization in Cenozoic magmatic arcs of Southeast Asia and the West Pacific: *Economic Geology* 100th anniversary volume 891, 930.
- Gertisser, R., Self, S., Thomas, L.E., Handley, H.K., Van Calsteren, P., Wolff, J.A., 2012. Processes and timescales of magma genesis and differentiation leading to the great Tambora eruption in 1815. *J. Petrol.* 53 (2), 271–297.
- Gomez-Tuena, A., Langmuir, C.H., Goldstein, S.I., Straub, S.M., Ortega-Gutiérrez, F., 2007. Geochemical evidence for slab melting in the Trans-Mexican Volcanic Belt. *J. Petrol.* 48 (3), 537–562.
- Hall, R., and Spakman, W., 2015. Mantle structure and tectonic history of SE Asia: *Tectonophysics*, 658, p. 14–45.
- Handley, H.K., Turner, S., Macpherson, C.G., Gertisser, R., and Davidson, J.P., 2011. Hf-Nd isotope and trace element constraints on subduction inputs at island arcs: Limitations of Hf anomalies as sediment input indicators: *Earth and Planetary Science Letters*, 304, no. 1–2, p. 212–223.
- Harris, C.W., Miller, M.S., Supendi, P., Widiyantoro, S., 2020. Subducted Lithospheric Boundary Tomographically Imaged Beneath Arc-Continent Collision in Eastern Indonesia. *J. Geophys. Res.* 125 (8), e2019JB018854.
- Harrison, R.L., Maryono, A., Norris, M.S., Rohrlach, B.D., Cooke, D.R., Thompson, J.M., Creaser, R.A., Thiede, D.S., 2018. Geochemistry of the Tumpangpitu porphyry Au-Cu-Mo and high-sulfidation epithermal Au-Ag-Cu deposit: Evidence for pre-and postmineralization diatremes in the Tujuh Bukit district, Southeast Java. In: *Indonesia: Economic Geology*, 113, pp. 163–192.
- Hayes, G.P., Moore, G.L., Portner, D.E., Hearne, M., Flamme, H., Furtney, M., Smoczyk, G.M., 2018. Slab2, a comprehensive subduction zone geometry model: *Science* 362 (6410), 58–61.
- Heuret, A., Lallemand, S., 2005. Plate motions, slab dynamics and back-arc deformation: *Physics of the Earth and Planetary Interiors* 149 (1–2), 31–51.
- Hoffer, G., Eissen, J.P., Beate, B., Bourdon, E., Fornari, M., Cotten, J., 2008. Geochemical and petrological constraints on rear-arc magma genesis processes in Ecuador: The Puyo cones and Mera lavas volcanic formations. *J. Volcanol. Geotherm. Res.* 176 (1), 107–118.
- Hollings, P., Cooke, D.R., Waters, P.J., Cousens, B., 2011. Igneous geochemistry of mineralized rocks of the Baguio district, Philippines: Implications for tectonic evolution and the genesis of porphyry-style mineralization: *Economic Geology* 106 (8), 1317–1333.
- Holm, R.J., Tapster, S., Jelsma, H.A., Rosenbaum, G., Mark, D.F., 2019. Tectonic evolution and copper-gold metallogenesis of the Papua New Guinea and Solomon Islands region. *Ore Geol. Rev.* 104, 208–226.
- Hoogewerff, J.A., Van Bergen, M., Vroon, P., Hertogen, J., Wordel, R., Sneyers, A., Nasution, A., Varekamp, J., Moens, H., Mouchel, D., 1997. U-series, Sr-Nd-Pb isotope and trace-element systematics across an active island arc-continent collision zone: Implications for element transfer at the slab-wedge interface. *Geochim. Cosmochim. Acta* 61 (5), 1057–1072.
- Hughes, G.R., Mahood, G.A., 2008. Tectonic controls on the nature of large silicic calderas in volcanic arcs: *Geology* 36 (8), 627–630.
- Hutchings, S.J., Mooney, W.D., 2021. The seismicity of Indonesia and tectonic implications: *Geochemistry. Geochem. Geophys. Geosyst.* 22 (9), e2021GC009812.
- Jacob, J., Dymnt, J., Yatheesh, V., 2014. Revisiting the structure, age, and evolution of the Wharton Basin to better understand subduction under Indonesia. *J. Geophys. Res.* 119 (1), 169–190.
- Jiang, C., Zhang, P., White, M.C., Pickle, R., Miller, M.S., 2022. A detailed earthquake catalog for Banda Arc-Australian plate collision zone using machine-learning phase picker and an automated workflow. *The Seismic Record* 2 (1), 1–10.
- Kirchenbaur, M., Schuth, S., Barth, A., Luguet, A., König, S., Idrus, A., Garbe-Schönberg, D., Münker, C., 2022. Sub-arc mantle enrichment in the Sunda rear-arc inferred from HFSE systematics in high-K lavas from Java. *Contrib. Mineral. Petrol.* 177 (1), 1–25.
- Kopp, H., Weinrebe, W., Ladage, S., Barckhausen, U., Klaeschen, D., Flueh, E.R., Gaedicke, C., Djajadihardja, Y., Grevenmeyer, I., Krabbenhoft, A., 2008. Lower slope morphology of the Sumatra trench system. *Basin Res.* 20 (4), 519–529.
- Koulakov, I., Kasatkina, E., Shapiro, N.M., Jaupart, C., Vasilevsky, A., El Khrepy, S., Al-Arif, N., Smirnov, S., 2016. The feeder system of the Toba supervolcano from the slab to the shallow reservoir. *Nat. Commun.* 7 (1), 1–12.
- Labanieh, S., Chauvel, C., Germa, A., Quidelleur, X., 2012. Martinique: a clear case for sediment melting and slab dehydration as a function of distance to the trench. *J. Petrol.* 53 (12), 2441–2464.
- Lee, C.T.A., Tang, M., 2020. How to make porphyry copper deposits. *Earth Planet. Sci. Lett.* 529, 115868.
- Lehnert, K., Su, Y., Langmuir, C., Sarbas, B., Nohl, U., 2000. A global geochemical database structure for rocks: *Geochemistry, Geophysics, Geosystems* 1 (5).
- Li, C.F., Wang, J., 2016. Variations in Moho and Curie depths and heat flow in Eastern and Southeastern Asia. *Marine Geophysical Research* 37 (1), 1–20.
- Lin, J.Y., Hsu, S.K., Sibuet, J.C., 2004. Melting features along the Ryukyu slab tear, beneath the southwestern Okinawa Trough. *Geophys. Res. Lett.* 31 (19).
- Liu, S., Suardi, I., Xu, X., Yang, S., Tong, P., 2021. The geometry of the subducted slab beneath Sumatra revealed by regional and teleseismic traveltimes tomography. *J. Geophys. Res.* 126 (1), e2020JB020169.
- Malawani, M.N., Lavigne, F., Gomez, C., Mutaqin, B.W., Hadmoko, D.S., 2021. Review of local and global impacts of volcanic eruptions and disaster management practices: the Indonesian example. *Geosciences* 11 (3), 109.
- Maryono, A., Harrison, R.L., Cooke, D.R., Rompo, I., Hoschke, T.G., 2018. Tectonics and geology of porphyry Cu-Au deposits along the eastern Sunda magmatic arc. *Indonesia: Economic Geology* 113 (1), 7–38.
- McCulloch, M.T., Gamble, J., 1991. Geochemical and geodynamical constraints on subduction zone magmatism. *Earth Planet. Sci. Lett.* 102 (3–4), 358–374.

- McLeod, O., Brenna, M., Briggs, R., Pittari, A., 2022. Slab tear as a cause of coeval arc-intraplate volcanism in the Alexandra Volcanic Group, New Zealand: *Lithos* 408, 106564.
- Menant, A., Sternai, P., Jolivet, L., Guillou-Frottier, L., Gerya, T., 2016. 3D numerical modeling of mantle flow, crustal dynamics and magma genesis associated with slab roll-back and tearing: The eastern Mediterranean case. *Earth Planet. Sci. Lett.* 442, 93–107.
- Miller, M.S., Zhang, P., Dahlquist, M.P., West, A.J., Becker, T.W., and Harris, C., 2021. Inherited lithospheric structures control arc-continent collisional heterogeneity: *Geology*.
- Moyen, J.F., 2009. High Sr/Y and La/Yb ratios: the meaning of the “adakitic signature”. *Lithos* 112 (3-4), 556–574.
- Newhall, C., Self, S., Robock, A., 2018. Anticipating future Volcanic Explosivity Index (VEI) 7 eruptions and their chilling impacts. *Geosphere* 14 (2), 572–603.
- Nicholls, I., Whitford, D., 1983. Potassium-rich volcanic rocks of the Muriah complex, Java, Indonesia: products of multiple magma sources? *J. Volcanol. Geotherm. Res.* 18 (1-4), 337–359.
- Peccerillo, A., 2017. Cenozoic Volcanism in the Tyrrhenian Sea Region. Springer.
- Planert, L., Kopp, H., Lueschen, E., Mueller, C., Flueh, E., Shulgin, A., Djajadihardja, Y., Krabbenhoft, A., 2010. Lower plate structure and upper plate deformational segmentation at the Sunda-Banda arc transition, Indonesia. *J. Geophys. Res.* 115, B8.
- Rosenbaum, G., Caulfield, J.T., Ubide, T., Ward, J.F., Sandiford, D., Sandiford, M., 2021. Spatially and Geochemically Anomalous Arc Magmatism: Insights From the Andean Arc: *Geochemistry, Geophysics, Geosystems*, e2021GC009688.
- Rosenbaum, G., Gasparon, M., Lucente, F.P., Peccerillo, A., Miller, M.S., 2008. Kinematics of slab tear faults during subduction segmentation and implications for Italian magmatism. *Tectonics* 27 (2).
- Rosenbaum, G., Mo, W., 2011. Tectonic and magmatic responses to the subduction of high bathymetric relief. *Gondwana Res.* 19 (3), 571–582.
- Rosenbaum, G., Sandiford, M., Caulfield, J., Garrison, J.M., 2019. A trapdoor mechanism for slab tearing and melt generation in the northern Andes. *Geology* 47 (1), 23–26.
- Ruscitto, D.M., Wallace, P.J., Cooper, L.B., Plank, T., 2012. Global variations in H₂O/Ce: 2. Relationships to arc magma geochemistry and volatile fluxes: *Geochemistry, Geophysics, Geosystems* 13 (3).
- Sandiford, M., 2008. Seismic moment release during slab rupture beneath the Banda Sea. *Geophys. J. Int.* 174 (2), 659–671.
- Schmidt, M.W., Poli, S., 1998. Experimentally based water budgets for dehydrating slabs and consequences for arc magma generation. *Earth Planet. Sci. Lett.* 163 (1-4), 361–379.
- Seton, M., Müller, R.D., Zahirovic, S., Williams, S., Wright, N.M., Cannon, J., Whittaker, J.M., Matthews, K.J., McGirr, R., 2020. A Global Data Set of Present-Day Oceanic Crustal Age and Seafloor Spreading Parameters: *Geochemistry, Geochem. Geophys. Geosyst.* 21 (10), e2020GC009214.
- Singer, D.A., 1995. World class base and precious metal deposits; a quantitative analysis. *Econ. Geol.* 90 (1), 88–104.
- Stolz, A., Varne, R., Wheller, G., Foden, J., Abbott, M., 1988. The geochemistry and petrogenesis of K-rich alkaline volcanics from the Batu Tara volcano, eastern Sunda arc. *Contrib. Mineral. Petrol.* 98 (3), 374–389.
- Suhendro, I., Toramaru, A., Miyamoto, T., Miyabuchi, Y., Yamamoto, T., 2021. Magma chamber stratification of the 1815 Tambora caldera-forming eruption. *Bull. Volcanol.* 83 (10), 1–20.
- Sushchevskaya, N., Levchenko, O., Dubinin, E., Belyatsky, B., 2016. Ninetyeast ridge: Magmatism and geodynamics. *Geochem. Int.* 54 (3), 237–256.
- Syracuse, E.M., van Keeken, P.E., Abers, G.A., 2010. The global range of subduction zone thermal models. *Phys. Earth Planet. Inter.* 183 (1-2), 73–90.
- Turner, S., Foden, J., 2001. U, Th and Ra disequilibria, Sr, Nd and Pb isotope and trace element variations in Sunda arc lavas: predominance of a subducted sediment component. *Contrib. Mineral. Petrol.* 142 (1), 43–57.
- Turner, S., Foden, J., George, R., Evans, P., Varne, R., Elburg, M., Jenner, G., 2003. Rates and processes of potassic magma evolution beneath Sangeang Api volcano, East Sunda arc, Indonesia. *J. Petrol.* 44 (3), 491–515.
- Van Bergen, M., Vroon, P., Varekamp, J., Poorter, R., 1992. The origin of the potassic rock suite from Batu Tara volcano (East Sunda Arc, Indonesia). *Lithos* 28 (3-6), 261–282.
- Vigouroux, N., Wallace, P.J., Williams-Jones, G., Kelley, K., Kent, A.J., Williams-Jones, A.E., 2012. The sources of volatile and fluid-mobile elements in the Sunda arc: A melt inclusion study from Kawah Ijen and Tambora volcanoes. *Indonesia: Geochemistry, Geophysics, Geosystems* 13 (9).
- Ward, J.F., Rosenbaum, G., Ubide, T., Wu, J., Caulfield, J.T., Sandiford, M., Gürer, D., 2021. Geophysical and geochemical constraints on the origin of Holocene intraplate volcanism in East Asia. *Earth Sci. Rev.*, 103624.
- Wehner, D., Rawlinson, N., Greenfield, T., Miller, M.S., Supendi, P., Liú, C., Widiyantoro, S., 2022. SASSIER22: Full-Waveform Tomography of the Eastern Indonesian Region That Includes Topography, Bathymetry, and the Fluid Ocean: *Geochemistry, Geophys., Geosyst.* 23 (11), e2022GC010563.
- Wilkinson, J.J., 2013. Triggers for the formation of porphyry ore deposits in magmatic arcs. *Nat. Geosci.* 6 (11), 917.
- Yang, S., Humayun, M., Salters, J., 2018. Elemental systematics in MORB glasses from the Mid-Atlantic Ridge: *Geochemistry, Geochem. Geophys. Geosyst.* 19 (11), 4236–4259.
- Yu, Y., Huang, X.L., Chung, S.L., Li, J., Lai, Y.M., Setiawan, I., Sun, M., 2022. Molybdenum isotopic constraint from Java on slab inputs to subduction zone magmatism. *Geochim. Cosmochim. Acta* 332, 1–18.
- Zhang, P., Miller, M.S., Eakin, C.M., 2022. Unraveling an enigmatic boundary along the Sunda-Banda volcanic arc. *Earth Planet. Sci. Lett.* 599, 117860.